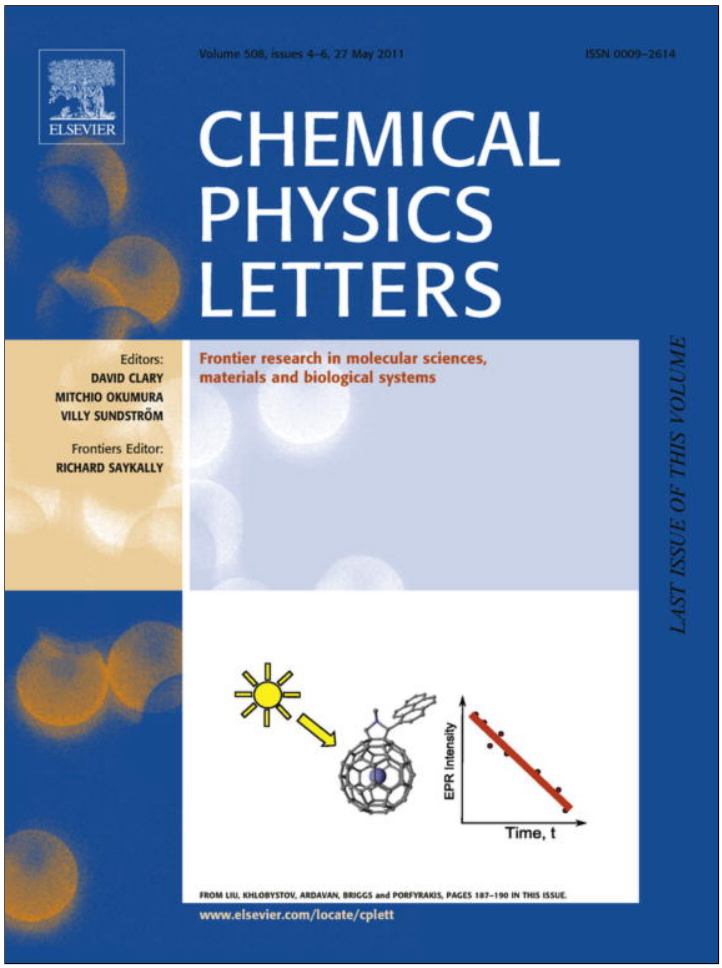

Chemical Physics Letters 508 (2011) 219–223

Contents lists available at ScienceDirect

Chemical Physics Letters

journal homepage: www.elsevier.com/locate/cplett

Computational surface chemistry of glycine on Si(1 1 1)7×7 and Si(1 0 0)2×1: Dissociative adsorption through adduct formation

A. Chatterjee, L. Zhang, K.T. Leung *

WATLab, Department of Chemistry and University of Waterloo, Waterloo, Ontario, Canada N2L 3G1

ARTICLE INFO

Article history:
Received 2 March 2011
In final form 15 April 2011
Available online 19 April 2011

ABSTRACT

Glycine adsorption on Si(1 1 1)7×7 and Si(1 0 0)2×1 model surfaces are studied by using Density Functional Theory (DFT) calculations. The present work illustrates that the formation of different surface adducts involving the $-NH_2$ and –COOH functional groups plays a vital role in determining the adsorbate structures on the 7×7 and 2×1 surfaces. No Si←O surface adduct can be obtained on Si(1 1 1)7×7, in marked contrast to Si(1 0 0)2×1, on which the formation of Si–O bond readily leads to O–H dissociative product. For Si(1 1 1)7×7, the existence of only Si←N adduct leads to N–H dissociative product and the formation of Si–N bond. These results are in good agreement with the experiment.

1. Introduction

Surface chemistry of organic materials on semiconductor surfaces has attracted a lot of recent attention from different disciplines in science and engineering. Understanding the intricate surface reactions and processes is fundamentally important to the development of novel engineered materials, biosensors, [1–4] and catalysts [5–7] used in chemical and pharmaceutical industries, biotechnology, and nanotechnology [8]. Incorporation of simple biomolecules, proteins, peptides and DNA molecules onto appropriate substrate surfaces, i.e. biofunctionalization, represents an essential step in the development of next-generation biodevices in nanobiotechnology and nanomedicine.

As the smallest building blocks of proteins and peptides, amino acids provide the basis to understand larger biomolecular systems. A number of recent studies have been reported on the adsorption of amino acids on different surfaces [9–13]. Among the notable semiconductor surfaces, Si(1 1 1)7×7 and Si(1 0 0)2×1 offer unique bonding sites, each providing one and two directional dangling bonds, respectively, for interactions with approaching molecules. These fundamental differences account for the different chemical selectivities of these Si surfaces towards different adsorbates. Understanding the interactions between amino acid molecules and these Si surfaces is therefore technologically important for the development of future biodevices. As the simplest naturally occurring amino acid, glycine (NH_2CH_2COOH) also represents a unique type of bifunctional molecules, with an amino ($-NH_2$) and a carboxylic acid (–COOH) groups. The study of glycine on Si surfaces is therefore especially important, because not only both the base and acid groups coexist in a single molecule but also these functional groups can be used to form hydrogen bonding adstructures. Appropriate coupling of these two functional groups to different surface sites offers surface selectivity for controlling the final adstructures. With one of the functional groups bonded to the surface and the other free to interact with incoming molecules, these bifunctional molecules are also important as linker molecules to form multilayer structures by hydrogen bonding for biodevice and molecular electronics applications [14].

To date, there are only four studies reported for glycine (and other amino acids) on Si(1 1 1)7×7 and Si(1 0 0)2×1 surfaces [15–18] and a recent computational work on Si(1 0 0)-c(4 × 2) surface [19]. The adsorption of glycine on Si(1 0 0)2×1 surface has been investigated by Lopez et al. [15] using high resolution electron energy loss spectroscopy (HREELS). The authors concluded that glycine adsorption mainly occurs via dissociation of the O–H bond of the carboxylic acid group and formation of O–Si bond, instead of dissociation of the N–H bond in the amino group and formation of N–Si bond. In a separate computational work, Qu et al. [16] later showed that on Si(1 0 0)2×1 the formation of O–Si bond is preferred over the formation of N–Si bond both thermodynamically (with the former producing a more negative adsorption energy than the latter) and kinetically (with N–H bond dissociation requiring more activation energy than O–H bond dissociation). This reaction has been proposed to go through an initial trapping step involving the formation of a datively bonded adduct. Qu et al. also showed that the adsorption energy of the Si←N adduct is much less than that of the Si←O adduct. This is not surprising in the formation of the initial adduct because the lone-pair

* Corresponding author. Address: Department of Chemistry, University of Waterloo, 200 University Ave. West, Waterloo, Ontario, Canada N2L 3G1. Fax: +1 (519) 746 0435.
E-mail address: tong@uwaterloo.ca (K.T. Leung).

0009-2614/$ - see front matter © 2011 Elsevier B.V. All rights reserved.
doi:10.1016/j.cplett.2011.04.057

electrons of the nitrogen atom in the amino group are more readily available for donation to a Lewis acid (e.g., a Si dangling-bond site) than that of the oxygen atom. Qu et al. further concluded that the lower O–H bond dissociation energy and the larger O–Si bond strength lead to 100% selectivity towards the formation of O–H dissociative product of glycine on Si(1 0 0)2×1 [16]. For glycine adsorption on Si(1 1 1)7×7 surfaces, Huang et al. [17], using HREELS and X-ray photoelectron spectroscopy (XPS), found that both the amino and carboxylic acid groups of glycine undergo reaction with the Si surface, and they concluded that these reactions lead to the formation of a bidentate adstructure that bridges two adatoms of the 7×7 unit cell. Realizing that the adatom-to-adatom separation (>6.65 Å) appears physically too large for simultaneous bidentate bonding through the $-NH_2$ and –OH termini of a glycine molecule (with a separation of 4.44 Å), we recently reexamined the adsorption process of glycine on Si(1 1 1)7×7 as a function of exposures with XPS [18]. We concluded that glycine adsorbs in an unidentate fashion to a single Si adatom by N–H bond dissociation of the amino group and formation of N–Si bond. The contrasting results obtained for the adsorption of glycine on the two different Si surfaces, i.e. Si(1 1 1)7×7 vs Si(1 0 0)2×1, demonstrate the remarkable differences in the chemical selectivities of the Si surfaces as dictated by their different local bonding structures.

In the dimer–adatom-stacking-fault model proposed by Takayanagi et al. [20], the 7×7 unit cell consists of 12 adatoms (in the topmost layer), six restatoms (in the next layer) and one corner-hole-atom (in the third layer), each with a dangling bond (an unsaturated valency), thereby reducing the total number of dangling bonds from 49 in the unreconstructed surface to 19 in the reconstructed surface. The adatom–restatom pair (with the adatom-to-restatom separation of 4.57 Å) provides the most important reaction site, because the smaller organic molecules, including glycine, have similar dimensions [21]. Furthermore, the adatom is reported to have less electron occupancy than the restatom due to a small charge transfer from the adatom to the restatom, resulting in formal charges of +7/12 for the corner adatom and −1 for the restatom [22]. Consequently, the topmost layer of the Si(1 1 1)7×7 surface (with the adatoms) is more electrophilic in nature, in contrast to the nucleophilic next layer with the restatoms. Because a center adatom has two neighboring restatoms, it has even less electron occupancy and is therefore more electrophilic than the corner adatom. The electrophilic adatoms should therefore be more reactive towards a nucleophilic functional group (e.g. $-NH_2$ of glycine) than the restatoms.

The Si(1 0 0)2×1 reconstruction, on the other hand, involves the formation of asymmetric buckled dimers on the surface. In this buckled dimer model for the Si(1 0 0)2×1 surface, one of the dangling bonds from each of two neighboring atoms forms a strong σ bond with each other, while the remaining dangling bond combines with that of a neighboring atom to form a weak π bond, creating a Si–Si dimer [23,24]. Due to the thermal motion at room temperature, the dimer is buckled with a dynamical tilt that causes an asymmetric electron distribution [25]. Charge transfer from the down-atom to the up-atom of the buckled dimer leads to the formation of an electrophilic–nucleophilic pair [23,26]. This structure of nucleophilic top layer (of the up-atoms) followed by an electrophilic second layer (of the down-atoms) is in marked contrast to the case of Si(1 1 1)7×7 surface. The difference in their electronic environments leads to different surface reactions, resulting in their selectivities towards specific organic molecules with different functional groups [21,26]. In the present work, we use ab initio calculations based on the Density Functional Theory (DFT) to demonstrate the importance of these basic chemistry concepts, particularly the formation of a viable adduct, in the adsorption of glycine on Si(1 1 1)7×7 and Si(1 0 0)2×1 surfaces.

2. Computational details

All the calculations have been performed at the DFT level with the hybrid B3LYP functional using the GAUSSIAN 09 software package [27]. The hybrid B3LYP functional consists of Becke's 3-parameter gradient-corrected exchange functional [28] and Lee–Yang–Parr correlation functional [29]. The B3LYP functional has been found to provide generally good agreement with experimental results for the adsorption of organic molecules on different surfaces [23,30–32]. In the present work, we have performed the calculations using four different split-valence basis sets. The 6-31G(d) basis set has been reported to provide similar results, particularly for equilibrium structure and frequency calculations for organic adsorbates, but at a lower computational cost when compared to the larger basis sets, including 6-31G+(d), 6-31G++(d), 6-31G+(d,p) and 6-31G++(d,p) [31].

Starting with an appropriately constructed test structure, we perform geometry optimization at B3LYP/6-31G(d) level to obtain a plausible equilibrium structure, which is used in a subsequent frequency calculation in order to determine whether the 'converged' structure is a true minimum. Transition states are located on the potential energy surface by using the combined quadratic Synchronous Transit-Guided Quasi–Newton method [33] in the GAUSSIAN 09 suite of programs. After obtaining the transition states at the B3LYP/6-31G(d) level, the structures of the transition states are then checked by the Intrinsic Reaction Coordinate calculations, and frequency calculations are performed to verify that only one imaginary frequency exists for the transition state.

Due to the complexity of the dimer–adatom-stacking-fault model structure of Si(1 1 1)7×7, a $Si_{16}H_{18}$ cluster is used in the present work to simulate one adatom–restatom pair of the 7×7 surface [34]. The $Si_{16}H_{18}$ cluster consists of one adatom (in the topmost layer) and one restatom (in the second top layer), with the pedestal atoms forming the third layer, and an additional fourth layer as the base layer to provide better rigidity to the cluster than the commonly used Si_9H_{12} cluster. With the exception of the adatom and restatom, the Si atoms in the perimeter of the cluster are terminated with H atoms. Due to the presence of unsaturated dangling bonds on the adatom and restatom, we fix the adatom–restatom separation in the $Si_{16}H_{18}$ cluster to that of the 7×7 unit cell (4.57 Å) during geometry optimization in order to avoid an unrealistic physical structure for the bare Si model surface. Once the optimized geometry of the bare $Si_{16}H_{18}$ cluster is obtained, subsequent geometry optimizations for a glycine molecule adsorbed on the cluster are performed without any geometrical constraints on the cluster and the glycine molecule.

To model the Si(1 0 0)2×1 surface, we use a double-dimer cluster ($Si_{15}H_{16}$), which has been reported to provide better results for the adsorption structures of a number of organic molecules [31] than the single-dimer cluster (Si_9H_{12}) [25,35,36]. The use of the double-dimer cluster could also facilitate the study of the dimer buckling effect and inter-dimer interactions, which cannot be realized in the single-dimer model. In order to build the $Si_{15}H_{16}$ cluster, we start by fixing the positions of the Si atoms by using the appropriate crystallographic data for the bulk and surface [35,37]. The Si atoms in the perimeter, except for the double-dimer atoms, are terminated with H atoms. The structure is then fully optimized without applying any constraints on the Si cluster. This optimized Si cluster is subsequently used for determining the adstructure of glycine, without any geometrical constraints on both glycine and the Si cluster.

The adsorption energy (ΔE) for an adstructure is calculated as the difference between the total energies of the optimized adstructure ($E_{adstructure}$) and the sum of the total energies of glycine ($E_{glycine}$) and the Si cluster ($E_{cluster}$), i.e. $\Delta E = E_{adstructure} - (E_{glycine} + E_{cluster})$, using the same level of theory [DFT/B3LYP/6-31G(d)]. All the total

energies are obtained without zero point energy corrections and no basis set superposition errors are made to ΔE.

3. Results and discussion

Figure 1a shows the potential energy diagram along with the adsorption energies of glycine on the $Si_{16}H_{18}$ cluster, and the respective optimized geometries of the adstructures. As the unreacted glycine molecule with the amino group oriented towards the Si adatom approaches the cluster, the N-to-Si separation is reduced. At a N-to-Si separation of 1.95 Å, a stable Si←N adduct state (II, with $\Delta E = -107.5$ kJ mol^{-1}) with respect to the unreacted state (I) can be obtained by appropriate geometry optimization. From this stable adduct state to the final N–H dissociative adsorption state (IV, with $\Delta E = -237.9$ kJ mol^{-1}), a transition state (III, with $\Delta E = -78.3$ kJ mol^{-1}) involving N–H bond dissociation can be observed at a N-to-Si separation of 1.83 Å. The corresponding N–H bond length in glycine is found to increase from 1.01 Å in the unreacted glycine molecule (I) to 1.05 Å in the adduct state (II) and to 1.31 Å in the transition state (III), which marks the on-set of N–H bond dissociation. In the final N–H dissociative adsorption state (IV), the N-to-Si separation becomes the N–Si bond (1.70 Å). The evolution of increasing N–H bond length with decreasing N-to-Si separation illustrates the process of N–H bond dissociation and concomitant N–Si bond formation. The presence of the stable Si←N adduct (II), as an intermediate state trapped between the unre-

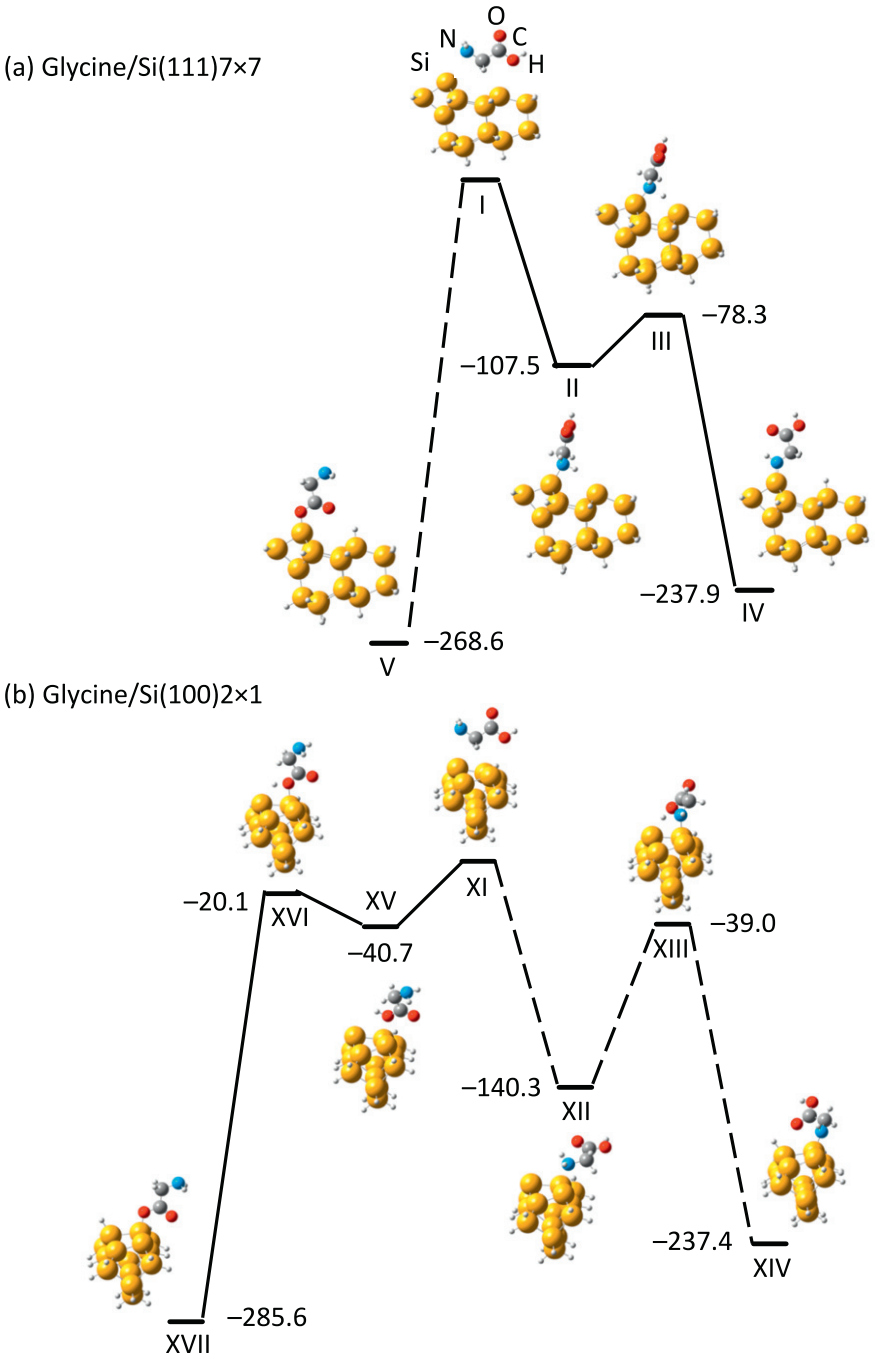

Figure 1. Potential energy diagram, along with the optimized geometries and adsorption energies (in kJ mol^{-1}) for different states, of glycine adsorption on model surfaces of (a) Si(1 1 1)7×7 and (b) Si(1 0 0)2×1. The more (less) probable pathway is shown as a solid (dashed) line.

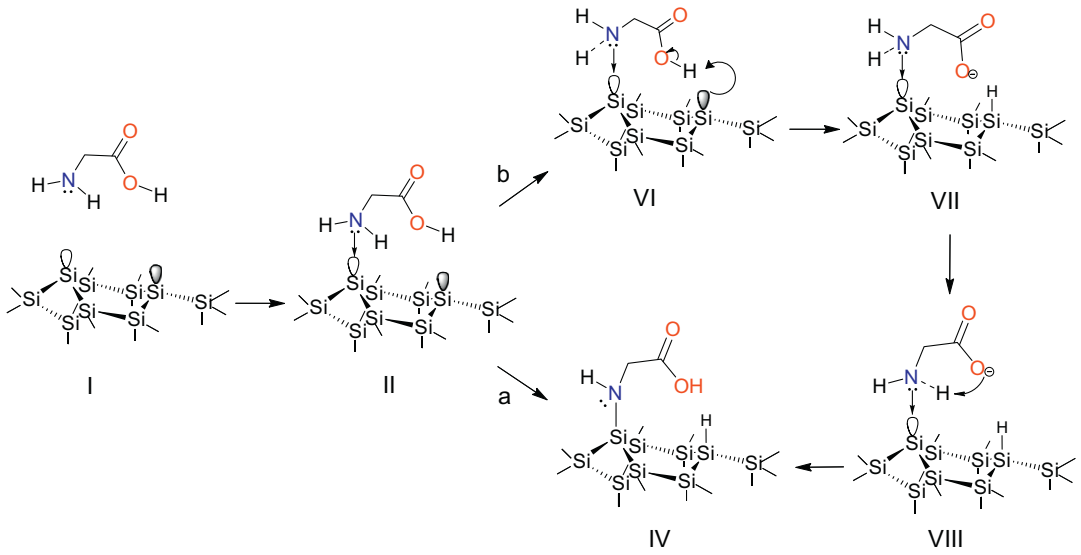

Figure 2. Schematic diagram of the adsorption of glycine on a model Si(1 1 1)7×7 surface, with direct proton transfer (route a) and with intramolecular proton transfer (route b) from a Si←N adduct (II), leading to the final adsorption state (IV).

acted and the final product states, is therefore essential in the formation of the final adsorption state.

We have also studied the corresponding pathway leading to the O–H dissociative adstructure (V, with $\Delta E = -268.6$ kJ mol^{-1}). An extensive search in the potential energy surface for an analogous Si←O adduct that involves dative bonding from the O atom of –OH or > C = O group of glycine to the Si adatom has been conducted. No stable adduct state is found. It should be noted that the adstructure V is obtained by geometry optimization of the pre-dissociated $NH_2CH_2COO\cdot$ and H· fragments attached, respectively, to the Si adatom and restatom. Although ΔE for the O–H dissociative adstructure appears more negative than that for N–H dissociative adstructure, the lack of a Si←O adduct indicates that such an adstructure cannot be realized. On the other hand, once the stable Si←N adduct is formed, the eventual proton transfer to the restatom from the Si←N adduct could proceed directly through the transition state, as shown in Figure 2, route a. In addition, an indirect intramolecular pathway, as illustrated in Figure 2, route b, could also occur because the energy barrier for intramolecular proton transfer for the zwitterionic glycine has been found to be quite low (less than 2.09 kJ mol^{-1}) [38]. The initial formation of a stable Si←N adduct (Figure 2, II) is also essential for the subsequent proton snatching step from the –COOH group by the nucleophilic restatom (Figure 2, VI). This is possible because the molecule is sufficiently long to reach the restatom after anchoring to the adatom. This can lead to the formation of the carboxylate anion, with the N atom in the amino group remaining datively bonded to the Si adatom (Figure 2, VII), and the eventual proton transfer from the amino moiety to the Si restatom (Figure 2, VIII). The plausibility of an intramolecular proton transfer to the carboxylate oxygen from the tetravalently bonded amino N atom has been evaluated in the case of isolated or gas-phase zwitterionic glycine molecule [38]. This intramolecular proton transfer could lead to the formation of the final N–Si bonded adstructure in an unidentate geometry as observed experimentally in our recent work [18].

Figure 1b shows the corresponding adsorption pathways of glycine on the model Si(1 0 0)2×1 surface involving N–H and O–H dissociation. Evidently, both the N–H and O–H dissociative pathways involve the formation of adduct states and transition states. In particular, as the N-to-Si separation decreases to 1.99 Å for the adduct state (XII, with $\Delta E = -140.3$ kJ mol^{-1}) and to 1.90 Å for the transition state (XIII, with $\Delta E = -39.0$ kJ mol^{-1}) and finally to 1.75 Å for the N–H dissociative adsorption state (XIV), the N–H bond length is found to increase concomitantly from 1.01 Å for the unreacted state (XI) to 1.03 Å for the adduct state (XII) and 1.41 Å for the transition state (XIII). Similarly, the O–H bond length increases from 0.98 Å for the unreacted state (XI) to 0.99 Å for the corresponding adduct state (XV, with $\Delta E = -40.7$ kJ mol^{-1}) and to 1.17 Å for the transition state (XVI, with $\Delta E = -20.1$ kJ mol^{-1}), as the O-to-Si separation decreases concomitantly to 2.05 Å (XV) and to 1.90 Å (XVI) and finally to 1.73 Å for the O–H dissociative adsorption state (XVII). As similarly observed for the Si(1 1 1)7×7 model surface (Figure 1a), the N–H dissociative adsorption state (XIV, with $\Delta E = -237.4$ kJ mol^{-1}) is found to be thermodynamically less stable than the O–H dissociative adsorption state (XVII, with $\Delta E = -285.6$ kJ mol^{-1}) for the Si(1 0 0)2×1 model surface. However, while a stable Si←O adduct cannot be obtained for the Si(1 1 1)7×7 model surface, the corresponding Si←N adduct (XII) is more stable than the Si←O adduct (XV) for the Si(1 0 0)2×1 model surface. Furthermore, the energy barrier between the Si←N adduct (XII) and the corresponding transition state (XIII), 101.3 kJ mol^{-1}, is considerably larger than that between Si←O adduct (XV) and its transition state (XVI), 20.6 kJ mol^{-1}. The smaller barrier found for the O–H dissociative pathway compared to the N–H dissociative pathway therefore also favors the formation of the O–H dissociative product (XVII) over the N–H dissociative product (XIV) kinetically. The formation of the O–H dissociative product via Si←O adduct formation for the Si(1 0 0)2×1 model surface is consistent with the calculated results reported by Qu et al. [16].

4. Concluding remarks

In the present work, we calculate the potential energy diagrams and the adsorption energies of relevant adstructures of glycine on $Si_{16}H_{18}$ and $Si_{15}H_{16}$ used, respectively, as model Si(1 1 1)7×7 and Si(1 0 0)2×1 surfaces. Dissociative adsorption of glycine on the two surfaces proceeds via the formation of the surface adduct states followed by the respective transition states that lead to the final adsorption states. For the Si(1 1 1)7×7 model surface,

the absence of a Si←O surface adduct leaves the formation of N–H dissociative product through the formation of the Si←N adduct as the only viable pathway. For the Si(1 0 0)2×1 model surface, the presence of the Si←O and Si←N surface adducts suggests that both O–H and N–H dissociative products are plausible. The considerably lower energy barrier to the respective transition state from the Si←O adduct than that from the Si←N adduct favors the formation of O–H dissociative adstructure. The present calculated result for the formation of N–H dissociative adstructure on the Si(1 1 1)7×7 surface is in good accord with the XPS data reported in our recent work [18], while the formation of O–H dissociative adstructure is also found to be in good agreement with the calculated results of Qu et al. [16] and the experimental data of Lopez et al. [15]. The present work therefore illustrates that the nature of the surface adduct is vitally important in controlling the selectivities of Si(1 1 1)7×7 and Si(1 0 0)2×1 towards the dissociative adsorption of glycine.

References

[1] A.J. Haes, R.V. Duyne, J. Am. Chem. Soc. 124 (2002) 10596.
[2] K. Pua, S. Dancil, D.P. Greiner, M.J. Sailor, J. Am. Chem. Soc. 121 (1999) 7925.
[3] F. Ricci et al., Biochemistry 76 (2009) 208.
[4] J.J. Gooding, Electroanalysis 14 (2002) 1149.
[5] J.L. Figueiredo, M.F.R. Pereira, Catal. today. 150 (2010) 2.
[6] R. Meyer, C. Lemire, Sh.K. Shaikhutdinov, H.J. Freund, Gold. Bull. 37 (2004) 72.
[7] C.T. Campbell, Annu. Rev. Phys. Chem. 41 (1990) 775.
[8] L. Grill, M. Dyer, L. Lafferentz, M. Person, M.V. Peters, S. Hecht, Nat. Nanotechnol. 2 (2007) 687.
[9] Q. Chen, N.V. Richardson, Nat. Mater. 2 (2003) 324.
[10] C. Huber, G. Wächtershäuser, Science 281 (1998) 670.
[11] R.L. Willett, K.W. Baldwin, K.W. West, L.N. Pfeiffer, PNAS 102 (2005) 7817.
[12] A. Rimola, M. Sodupe, P. Ugliengo, J. Phys. Chem. C 113 (2009) 5741.
[13] K. Odbadrakh, X. Luo, J.-G. Lee, C. Sagui, C. Roland, J. Phys. Chem. C 111 (2007) 12760.
[14] T. Rakshit, G.C. Liang, A.W. Ghosh, S. Dutta, Nano Lett. 4 (2004) 1803.
[15] A. Lopez, T. Heller, T. Bitzer, N.V. Richardson, Chem. Phys. 277 (2002) 1.
[16] Y.Q. Qu, Y. Wang, J. Li, K.L. Han, Surf. Sci. 569 (2004) 12.
[17] J.Y. Huang et al., Langmuir 23 (2007) 6218.
[18] L. Zhang, A. Chatterjee, K.T. Leung, J. Chem. Phys. 130 (2009) 121103.
[19] X. Luo, G. Qian, C. Sagui, C. Roland, J. Phys. Chem. C 112 (2008) 2640.
[20] K. Takayanagi, Y. Tanishiro, M. Takahashi, S. Takahashi, J. Vac. Sci. Technol. A 3 (1985) 1502.
[21] F. Tao, G.Q. Xu, Acc. Chem. Res. 37 (2004) 882.
[22] J.E. Northrup, Phys. Rev. Lett. 57 (1986) 154.
[23] A. Radi, M. Ebrahimi, K.T. Leung, Surf. Sci. 604 (2010) 1073.
[24] J. Yoshinobu, Prog. Surf. Sci. 77 (2004) 37.
[25] J. Li, Y.-Q. Qu, K.-L. Han, G.-Z. He, Surf. Sci. 586 (2005) 45.
[26] M.A. Filler, S.F. Bent, Prog. Surf. Sci. 73 (2003) 1.
[27] M.J. Frisch et al., Gaussian 09, Revision A.1, Gaussian Inc., Wallingford, CT, 2009.
[28] A.D. Becke, J. Chem. Phys. 98 (1993) 5648.
[29] C. Lee, W. Yang, R.G. Parr, Phys. Rev. B 37 (1988) 785.
[30] X.J. Zhou, Q. Li, Z.H. He, X. Yang, K.T. Leung, Surf. Sci. 543 (2003) L668.
[31] M. Ebrahimi, J.F. Rios, K.T. Leung, J. Phys. Chem. C 113 (2009) 281.
[32] Q. Li, K.T. Leung, Surf. Sci. 479 (2001) 69.
[33] C. Peng, H.B. Schlegel, Israel J. Chem. 33 (1993) 449.
[34] H.S. Lee, C.H. Choi, Theor. Chem. Acc. 120 (2008) 79.
[35] R. Felici, I.K. Robinson, C. Ottaviani, P. Imperatori, P. Eng, P. Perfetti, Surf. Sci. 375 (1997) 55.
[36] X. Lu, X. Xu, N. Wang, Q. Zhang, M.C. Lin, J. Phys. Chem. B 105 (2001) 10069.
[37] G. Celotti, D. Nobili, P. Ostoja, J. Mater. Sci. 9 (1974) 821.
[38] Y.-C. Tse, M.D. Newton, S. Vishveshwara, J.A. Pople, J. Am. Chem. Soc. 100 (1978) 4329.